The Astrophysical Journal, 645: L157–L160, 2006 July 10

MOTION OF 3–6 keV NONTHERMAL SOURCES ALONG THE LEGS OF A FLARE LOOP

Linhui Sui,[1,2] Gordon D. Holman,[2] and Brian R. Dennis[2]
Received 2006 April 24; accepted 2006 May 31; published 2006 July 7

ABSTRACT

Observations of nonthermal X-ray sources are critical to the study of electron acceleration and transport in solar flares. Strong thermal emission radiated from the preheated plasma before the flare impulsive phase often makes it difficult to detect low-energy X-ray sources that are produced by relatively low-energy nonthermal electrons. Knowledge of the distribution of these low-energy nonthermal electrons is particularly important in determining the total nonthermal electron energy in solar flares. We report on an "early impulsive flare" in which impulsive hard X-ray emission was seen early in the flare before the soft X-ray emission had risen significantly, indicating limited plasma preheating. Early in the flare, *RHESSI* <25 keV images show coronal sources that moved first downward and then upward along the legs of a flare loop. In particular, the 3–6 keV source appeared as a single coronal source at the start of the flare, and then it evolved into two coronal sources moving down along the two legs of the loop. After nearly reaching the two footpoints at the hard X-ray peak, the two sources moved back up to the looptop again. *RHESSI* images and light curves all indicate that nonthermal emission dominated at energies as low as 3–6 keV. We suggest that the evolution of both the spectral index and the low-energy cutoff of the injected electron distribution could result in the accelerated electrons reaching a lower altitude along the legs of the dense flare loop and hence result in the observed downward and upward motions of the nonthermal sources.

Subject headings: Sun: flares — Sun: particle emission — Sun: X-rays, gamma rays

Online material: color figure

1. INTRODUCTION

Because nonthermal X-rays in solar flares are produced by energetic electrons, observations of these sources are critical for studying particle acceleration and transport processes in flares. So far, several types of nonthermal X-ray sources have been discovered. *Yohkoh* Hard X-ray Telescope (HXT) observations showing simultaneously brightening (within 0.1 s) of two hard X-ray (HXR) footpoints (Sakao 1994) support a nonthermal footpoint scenario: electrons propagate from the top to the footpoints of flare loops, where they lose their energy and radiate the observed thick-target bremsstrahlung X-rays (Brown 1971). Masuda et al. (1994) reported >20 keV HXR coronal sources located above the soft X-ray (SXR) loops in a number of *Yohkoh* flares. The thermal interpretation for these above-the-looptop HXR sources proposed by Masuda et al. (1994) was ruled out because the rapid intensity variability was inconsistent with this interpretation (Hudson & Ryan 1995). Several nonthermal interpretations have been proposed (e.g., Wheatland & Melrose 1995; Fletcher 1995; Sui et al. 2002). Recently, observations of three homologous flares on 2002 April 14–16 obtained with *RHESSI* (Lin et al. 2002) showed that >25 keV HXRs were dominated by emissions from coronal sources near the looptop, instead of from the loop footpoints in typical flares (Sui et al. 2004). Veronig & Brown (2004) attributed these bright HXR looptop sources to thick-target bremsstrahlung from nonthermal electrons stopped in the corona due to a high loop column density.

We have selected a set of *RHESSI* flares in which impulsive (presumably nonthermal) HXR emission is seen early in the flare before the SXR emission has risen significantly, indicating very limited plasma preheating before electron acceleration. We call them "early impulsive flares." The original motivation for studying these flares was to search for evidence of a low-energy cutoff to the nonthermal electron distribution, which is critical in estimating the total nonthermal electron energy in flares (e.g., Holman 2003). Because of the relatively weak thermal emission, the nonthermal flux could dominate *RHESSI* X-ray spectra down to very low energies, in contrast to most flares, where the SXR emission rises well before the HXR emission. Therefore, the early impulsive flares offer the advantage that evidence for a low-energy cutoff can be identified at lower energies in the X-ray spectrum. Recently, Sui et al. (2005) reported that such evidence for a low-energy cutoff had been found in a number of early impulsive flares.

Early impulsive flares offer another advantage: nonthermal sources can be more easily detected in X-ray images when the thermal sources are relatively weak. In the more common flares, due to significant plasma heating, thermal emission from flare loops is strong when particle acceleration occurs. Because of the limited *RHESSI* dynamic range (~10 : 1), weak sources located outside the flare loops, such as the reported coronal sources above loops (Sui & Holman 2003; Sui et al. 2004; Veronig et al. 2006), are difficult to detect in the presence of the much stronger loop emission. Moreover, any nonthermal sources produced by energetic electrons as they propagate along flare loops would be hidden by emission from the electrons that have reached the footpoints and by stronger thermal emission from the same loop. Furthermore, with the existence of hot plasma in the loop, any nonthermal electrons with energies close to the thermal electron energies will be thermalized (Emslie 2003; Galloway et al. 2005). Therefore, we lose important information about these low-energy nonthermal electrons.

Here we report *RHESSI* observations of an early impulsive flare that show coronal sources below 25 keV moving downward and then upward along both legs of the loop during the impulsive phase of the flare. The implications of these new observations are discussed in § 3.

[1] Department of Physics, Catholic University of America, Washington, DC 20064.

[2] Laboratory for Solar and Space Physics, Code 612.1, NASA Goddard Space Flight Center, Greenbelt, MD 20771.

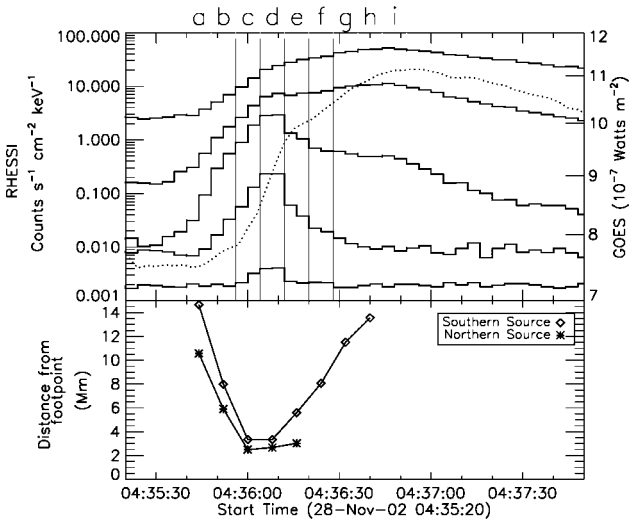

FIG. 1.—*Top*: *RHESSI* (*solid lines*) and *GOES* 1–8 Å (*dotted lines*) light curves. The *RHESSI* energy bands (*from top to bottom*) are 3–6, 6–12, 12–25, 25–50, and 50–100 keV, with corresponding scaling factors 5, 1, 4, 3, and 0.5, respectively. The *RHESSI* and *GOES* integration times are 4 and 3 s, respectively. The vertical lines indicate the start and end times of each 8 s interval (designated by the labels at the top) for each image shown in Fig. 2. *Bottom*: Distance between the 3 and 6 keV moving sources and their corresponding footpoints located in the 25–50 keV image (see Fig. 2) in the flare. The plotted distances were determined from the location of each source in the images taken to be the centroid within the 60% contour of the peak value. All distances are plane-of-sky values with no corrections for motions away from or toward the observer.

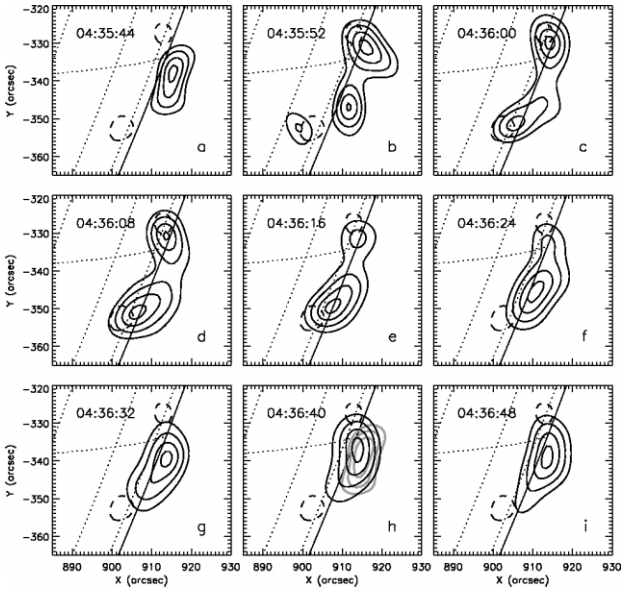

FIG. 2.—*RHESSI* 3–6 keV maps with solid contours at 40%, 60%, and 80% of the peak flux. To show the footpoint location, 80% contours of the peak flux (*dashed contours*) in the 25–50 keV image at 04:36:08 UT (interval d) are overlaid in each panel. *RHESSI* grids 3–9 were used for all images, giving a spatial resolution of ~7″. The integration time of each image is 8 s. The median time of the each interval (UT) is indicated. The image panel labels correspond to the interval labels marked in Fig. 1. In panel *h*, the 3–6 keV map at 04:35:44 UT (*gray contours*) is overlaid. The solid curve is the solar limb, and the dotted lines show solar longitude and latitude grids at 5° interval.

2. OBSERVATIONS AND DATA ANALYSIS

RHESSI observed a C1.1 flare on 2002 November 28 near the southwest solar limb (S18°W89°) starting at 04:35:30 UT. During the flare, the *RHESSI* attenuator status was A0; i.e., no attenuators were in front of the nine germanium detectors. Therefore, *RHESSI* was sensitive to energies as low as 3 keV (Smith et al. 2002). As indicated by the *RHESSI* light curves shown in Figure 1 (*top*), the start of the 25–50 keV flux increase was ~12 s delayed relative to the <25 keV energy bands. The *GOES* 1–8 Å flux started to increase at almost the same time as the *RHESSI* 25–50 keV started to increase, suggesting the absence of the significant plasma preheating usually seen early in flares. In typical flares the *GOES* SXR flux starts to increase well before the HXR flux.

The *RHESSI* 3–6 keV images (Fig. 2) show coronal sources moving along a flare loop. The first panel is the image at 04:35:40–04:35:48 UT (interval "a" in Fig. 1; hereafter, only the median time of each 8 s interval is stated). This is the time when the 25–50 keV flux started to increase. The image shows one extended coronal source above the southwest limb, which could be two sources unresolved by *RHESSI* at the ~4″ level. In order to show where the footpoints are located, we overlaid the 25–50 keV image (dashed contours) at the time of the HXR peak (interval d) when footpoints were seen by *RHESSI*. Evidently, the two footpoints were on the solar disk, although additional sources over the limb cannot be ruled out. In interval b (8 s later), the image apparently shows two separate coronal sources, both still above the limb but located lower than the coronal source seen earlier. The additional 3–6 keV source on the solar disk near (900″, −353″) is likely to be an artifact of the imaging process because it does not exist in images at other times and energy bands. Another 8 s later (interval c), the two coronal sources appeared to move along the two legs of the flare loop toward the footpoints. At the HXR peak time near 04:36:08 UT (interval d), the two sources remained at the same location as 8 s earlier, suggesting that these two sources had reached the their lowest altitude. It is evident that the footpoints seen in the 25–50 keV images are lower in altitude than the 3–6 keV sources.

After the HXR peak time, the two sources started to move back upward along the loop. The upward motion of the southern source is particularly evident from 04:36:08 to 04:36:24 UT (intervals d, e, and f). At 04:36:32 and 04:36:40 UT (intervals g and h), presumably because the northern source was too weak, only the southern coronal source can be identified in the images. The southern source continued to move toward the northwest, i.e., toward the top of the loop. The coronal source at those times had still not reached the top of the loop. After 04:36:40 UT, the location of the coronal source did not change as rapidly as before, implying that it had reached the looptop. It took ~32 s for the southern source to move from the bottom of the loop to the top. As seen in Figure 2*h*, the coronal source at this time was located lower than the original coronal source seen in Figure 2*a*. We found the centroid of the coronal source in Figure 2*h* to be ~1.″5 lower in altitude than that in Figure 2*a*. Although the image spatial resolution is about 7″, source centroids obtained with *RHESSI* can be located to an accuracy of better than 1″ (Hurford et al. 2002). After 04:36:40 UT, the coronal source moved outward (more toward the south) at a speed of ~10 km s^{-1}. This apparent looptop outward motion, similar to that reported by Tsuneta et al. (1992), Gallagher et al. (2002), and Sui & Holman (2003), presumably is evidence for loop formation at higher and higher altitudes due to continuous magnetic reconnection above the loops.

To quantitatively study the source motion along the two legs of the loop, we calculate the distances between the moving sources and their corresponding footpoints, i.e., the distance between the moving northern source and the northern 25–50 keV footpoint, and the distance between the moving southern

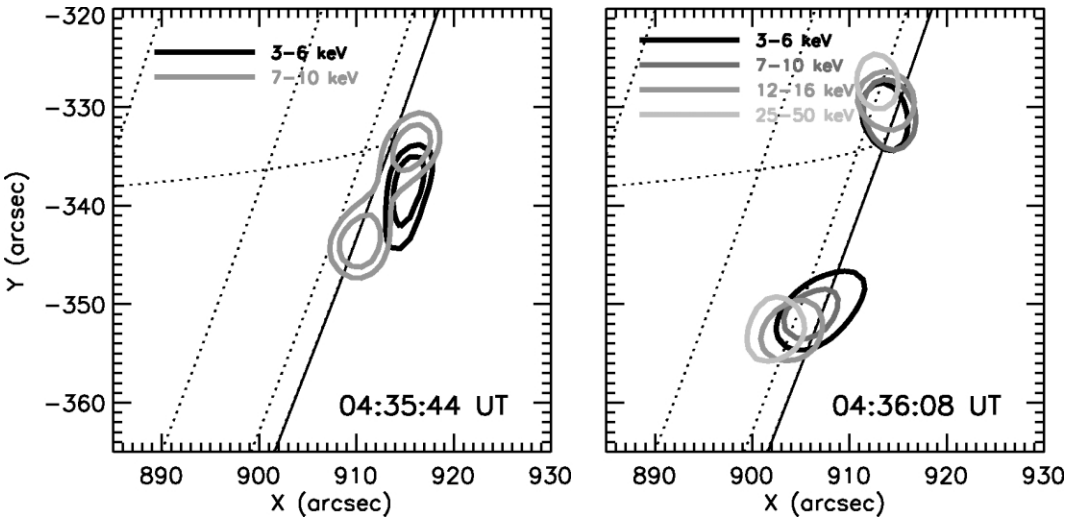

FIG. 3.—*RHESSI* images in multiple energy bands at 04:35:44 UT (interval a in Fig.1, *left*) and 04:36:08 UT (interval d in Fig.1, *right*). The contour levels are 80% and 90% of the peak flux of the image in each energy band for the left panel, and 80% of the peak fluxes for the right panel. [*See the electronic edition of the Journal for a color version of this figure.*]

source and the southern 25–50 keV footpoint. We do not know the shape of the loop or its orientation relative to the surface of the Sun. Thus, instead of calculating the distance along a loop, we calculate the distance by summing the linear distances between the neighboring sources, which were below the moving coronal source, all the way down to the footpoints. The results are shown in Figure 1 (*bottom*). The footpoints are taken as the two 25–50 keV sources seen in the image at the HXR peak of 04:36:08 UT (Fig. 2, *dashed contours*). The locations of the moving sources and the footpoints were taken to be the source centroid within 60% of the peak flux in each image.

At 04:35:44 UT (interval a), when there was only one coronal source, the distance between the coronal source and the northern and southern footpoints are both calculated. As indicated in Figure 1 (*bottom*), this coronal source was ~4 Mm (~5″.5) farther away from the southern footpoint than from the northern footpoint. This could be due to a projection effect, because the northern footpoint was located farther west, as indicated by the 25–50 keV image at the HXR peak. It could also be the result of the loop not being vertical or the source not being located exactly at the looptop.

From 04:35:52 to 04:36:16 UT, the 60% contours show two separate (southern and northern) sources. It is clear that both coronal sources moved downward toward their footpoints before 04:36:00 UT, at speeds of ~500 and 700 km s^{-1} for the northern and southern sources, respectively. Because we ignore the projection effect, the speeds we obtained are lower limits. At 04:36:00 and 04:36:08 UT, the two sources reached their minimum altitudes, which can be interpreted as the two footpoints at 3–6 keV. The 3–6 keV footpoints were still located ~3 Mm higher than the footpoints at 25–25 keV. During the period of 04:36:08–04:36:40 UT, the southern source moved away from the footpoint toward the looptop. The average upward speed was ~340 km s^{-1}, roughly half of the downward speed. Although only two data points are available, the northern source can also be seen to move away from the northern footpoint after 04:36:08 UT with a speed of ~45 km s^{-1}.

Similar downward and upward motions can also be seen in images at energies between 6 and 25 keV. On the basis of the source location change at different energies, we found that the lower the energy, the more evident the motion. Note that the early downward motion is different from the looptop downward motion recently discovered with *RHESSI* in which the single coronal source was always located at the looptop during the flare (Sui & Holman 2003; Sui et al. 2004; Veronig et al. 2006). After 04:36:40 UT, the *RHESSI* images below 25 keV all show a looptop coronal source, which also moved upward as seen in the 3–6 keV images. *RHESSI* >25 keV images, only available around the HXR peak times (intervals c and d), show two separated footpoints.

When the sources moved along the loop, the source altitudes at different energies were different at each time. The higher energy sources were always located lower in altitude than the lower energy sources. Two examples are shown in Figure 3. At 04:35:44 UT (Fig. 3, *left*), the single 3–6 keV coronal source is higher than the two coronal sources at 7–10 keV, which appeared to be located in the two legs of the flare loop. In the images at the HXR peak (Fig. 3, *right*), the higher energy sources (e.g., 25–50 keV) are consistently lower than the low-energy source (e.g., 3–6 keV) in both legs of the loop. Similar energy distribution of footpoint sources in another *RHESSI* event was reported by Aschwanden et al. (2002), but with footpoints seen at a lowest energy of 15 keV, not 3–6 keV as in this flare.

3. DISCUSSIONS

Two questions merit discussion here: Are the moving sources thermal or nonthermal? What causes their downward and upward motions along the flare loop?

The *RHESSI* and *GOES* light curves support the nonthermal interpretation down to low energies. The *GOES* 1–8 Å flux and *RHESSI* 25–50 keV flux began to increase almost simultaneously (within ~4s), which indicates that plasma preheating before the particle acceleration was minimal. Therefore, the nonthermal emission could dominate at low energies early in the flare. This is the reason why such motion can be detected in this flare. It is also likely that early in the flare the nonthermal emission also contributed to the *GOES* 1–8 Å flux, which is usually interpreted as thermal emission.

The *RHESSI* images also suggest that the moving X-ray sources were dominated by nonthermal, thick-target bremsstrahlung, even down to 3–6 keV. In more common flares,

RHESSI <25 keV images often show that the coronal sources at higher energies are located higher in altitude than the lower energies. These coronal sources are understood to be of thermal origin, and their energy distribution is in agreement with the standard flare model: the outer loops are newly reconnected and hotter, while the inner loops reconnected earlier and have cooled (Tsuneta et al. 1992). However, in this flare, we found that the low-energy sources (at both the looptop and the loop footpoints) are located higher than the high-energy sources (Fig. 3). This is qualitatively consistent with the collisional thick-target model (Brown et al. 2002): high-energy electrons propagate deeper into the dense solar atmosphere than low-energy electrons. In particular, the observation of one 3–6 keV coronal source at or above the looptop and two 7–10 keV sources in the two legs of the loop at 04:35:44 UT (Fig. 3, *left*) is what would be expected if accelerated electrons are injected at the top of a relatively dense loop.

Preliminary spectral analysis of this flare suggests the dominance of nonthermal emission at low energies down to 3 keV. Detailed spectral analysis of this flare is in preparation. Nonthermal emission extending to <5 keV has also been reported by Kane et al. (1992) from their analysis of flare spectra from 5 keV to 3.2 MeV obtained with the spectrometer on the *ICE/ISEE 3* spacecraft.

The single coronal source early in the flare (Fig. 2*a*) was located higher than the coronal source formed later (Fig. 2*h*). If the two coronal sources were both thermal looptop sources, then according to the standard flare model, the early coronal source should have been lower than the later one, not higher as observed. However, the altitude decrease of the looptop sources seen here may be related to the recently discovered looptop downward motions (Sui & Holman 2003; Sui et al. 2004; Veronig et al. 2006; Li & Gan 2005). The only difference is that the single coronal source seen early in this flare was nonthermal, while the looptop sources seen in those cases were thermal.

One likely explanation of the upward motion of the source after the HXR peak is that the plasma density increased inside the flare loop due to chromospheric evaporation. Similar gradual upward motion of X-ray sources along flare loops has been reported in a flare observed with *Yohkoh* HXT (Silva et al. 1997) and in several *RHESSI* events (Liu et al. 2006). Both Silva et al. (1997) and Liu et al. (2006) suggested that this upward motion could be explained as a result of plasma density buildup due to chromospheric evaporation. When the loop density increases, electrons will be stopped and radiate thick-target bremsstrahlung at higher and higher altitudes in the flare loop. But chromospheric evaporation cannot account for the downward motion early in the flare. In order to explain the downward motion, the plasma density inside the loop would have to decrease so that electrons can propagate farther down the loop. So far, no observations have indicated an early decrease in loop density in flares. Therefore, this explanation of the downward motion is unlikely.

The soft-hard-soft (SHS) spectral evolution often seen in impulsive flares (see Grigis & Benz 2004 and references therein) may contribute to both the downward and upward motions of nonthermal sources along the flare loop. Preliminary spectral analysis of this event reveals that its X-ray spectra have a SHS evolution pattern, indicating that the spectra of the emitting nonthermal electrons also have a SHS evolution. Assuming thick-target emission (Brown 1971), the electron spectral index was found to vary from ~ -6 to -4. When the electron spectra are soft early in the flare, the mean electron energy is low, and most of the electrons will lose their energy high in the loop due to the Coulomb collision with ambient plasma. When the spectra harden with time, the mean electron energy increases, and the electrons can travel farther down the loop before losing their energies, resulting in the early downward motion of the X-ray sources. After the HXR peak, the electron spectra become softer and the travel distance becomes shorter again, resulting in the later upward motion.

Another scenario that could also contribute to the source motions seen in this flare is a variation with time of the low-energy cutoff to the nonthermal electron distribution. Spectral analysis of early impulsive flares recently done by Sui et al. (2005) revealed that the nonthermal component of the photon spectra flattens below ~20–30 keV from its power-law distribution at higher energies. Spectral fitting with a bremsstrahlung thick-target model gives low-energy cutoffs in the electron distribution ranging from ~20 to 45 keV. Most interestingly, Sui et al. (2005) found that the low-energy cutoff correlated with the >25 keV HXR flux. The correlation between the electron low-energy cutoff and HXR flux was also reported by Gan et al. (2002) with BATSE *CGRO*. Before the time of the HXR peak, the value of the low-energy cutoff increases, so the power-law electron distribution is shifted to higher energies. Consequently, electron propagation distances increase, causing the early downward motion of the nonthermal source. After the HXR peak, the low-energy cutoff decreases, so the power-law electron distribution extends to lower energies. Consequently, electrons stop at higher and higher altitude in the loop, resulting in the upward motion.

REFERENCES

Aschwanden, M. J., Brown, J. C., & Kontar, E. P. 2002, Sol. Phys., 210, 383
Brown, J. C. 1971, Sol. Phys., 18, 489
Brown, J. C., Aschwanden, M. J., & Kontar, E. P. 2002, Sol. Phys., 210, 373
Emslie, A. G. 2003, ApJ, 595, L119
Fletcher, L. 1995, A&A, 303, L9
Gallagher, P. T., Dennis, B. R., Krucker, S., Schwartz, R. A., & Tolbert, A. K. 2002, Sol. Phys., 210, 341
Galloway, R. K., MacKinnon, A. L., Kontar, E. P., & Helander, P. 2005, A&A, 438, 1107
Gan, W.-Q., Li, Y.-P., & Chang, J. 2002, Chinese J. Astron. Astrophys., 2, 103
Grigis, P. C., & Benz, A. O. 2004, A&A, 426, 1093
Holman, G. D. 2003, ApJ, 586, 606
Hudson, H. S., & Ryan, J. 1995, ARA&A, 33, 239
Hurford, G. J., et al. 2002, Sol. Phys., 210, 61
Kane, S. R., McTiernan, J., Loran, J., Fenimore, E. E., Klebesadel, R. W., & Laros, J. G. 1992, ApJ, 390, 687
Li, Y.-P., & Gan, W.-Q. 2005, ApJ, 629, L137
Lin, R. P., et al. 2002, Sol. Phys., 210, 3
Liu, W., Liu, S., Jiang, Y., & Petrosian, V. 2006, ApJ, in press
Masuda, S., Kosugi, T., Hara, H., Tsuneta, S., & Ogawara, Y. 1994, Nature, 371, 495
Sakao, T. 1994, Ph.D. thesis, Univ. Tokyo
Silva, A. V. R., Wang, H., Gary, D. E., Nitta, N., & Zirin, H. 1997, ApJ, 481, 978
Smith, D. M., et al. 2002, Sol. Phys., 210, 33
Sui, L., & Holman, G. D. 2003, ApJ, 596, L251
Sui, L., Holman, G. D., & Dennis, B. R. 2004, ApJ, 612, 546
———. 2005, AGU Fall Meeting, abstract SH13A-0291
Sui, L., Holman, G. D., Dennis, B. R., Sam, K., Schwartz, R. A., & Tolbert, K. 2002, Sol. Phys., 210, 245
Tsuneta, S., Hara, H., Shimizu, T., Acton, L. W., Strong, K. T., Hudson, H. S., & Ogawara, Y. 1992, PASJ, 44, 63
Veronig, A. M., & Brown, J. C. 2004, ApJ, 603, L117
Veronig, A. M., Karlicky, M., Vrsnak, B., Temmer, M., Magdalenic, J., Dennis, B. R., Otruba, W., & Poetzi, W. 2006, A&A, 446, 675
Wheatland, M. S., & Melrose, D. B. 1995, Sol. Phys., 158, 283